

# Synchronization in Hierarchical Cluster Networks

Xingang Wang,<sup>1,2</sup> Liang Huang,<sup>3</sup> Ying-Cheng Lai,<sup>3</sup> and Choy Heng Lai<sup>4,2</sup>

<sup>1</sup>*Temasek Laboratories, National University of Singapore, Singapore, 117508*

<sup>2</sup>*Beijing-Hong Kong-Singapore Joint Centre for Nonlinear & Complex Systems (Singapore),  
National University of Singapore, Kent Ridge, Singapore, 119260*

<sup>3</sup>*Department of Electrical Engineering,*

*Arizona State University, Tempe, Arizona 85287, USA*

<sup>4</sup>*Department of Physics, National University of Singapore, Singapore, 117542*

(Dated: February 9, 2020)

## Abstract

For real cluster networks, the size of the clusters are usually nonidentical, very often it assumes a heterogeneous distribution. Using cluster's size as the proxy for its importance, a topological hierarchy will be formed in cluster networks. We study synchronization problem in this kind of hierarchical cluster networks and explore the effect of coupling gradient in promoting network synchronization. It is found that, for network of fixed topology and coupling cost, there exists an optimal coupling gradient where network synchronizability achieves its maximum. The optimal gradient is determined not only by the size distribution of the clusters, but also by the connectivity of the intra- and intercluster links. We develop a theoretical analysis to the dependence of the optimal gradient to the network parameters and propose a general scheme for constructing hierarchical network of stronger synchronizability. The theoretical predictions are verified by numerical simulations.

PACS numbers: 05.45.Xt, 05.45.Ra, 89.75.Hc

Cluster network refers to the kind of complex network in which nodes are joined together in tightly knit modules, between which there are only looser connections [1]. Since its first discovery in social and biological systems, there has been mounting evidences showing that cluster network is ubiquitous in real nature. Typical examples include the metabolic networks, the protein networks, and the neural networks [2]. To manifest the network functions, nodes are endowed with dynamics and studies on the collective behavior of complex networks have attracted much attention in recent years. One typical study is network synchronization, where nodes are usually chaotic oscillators and links are couplings, and investigations on the dependence of network synchronizability to network topology or coupling schemes now are prevailing over the nonlinear science [3]. Yet, comparing to the array of researches carried for the other types of networks, few attention has been paid to the synchronization of cluster networks. Due to its unique structure, the dynamical processes on cluster networks may have significant difference to the other types of networks, and is warranted with new features [4, 5].

In terms of synchronization, four basic quantities are normally used to characterize cluster networks: the number of intercluster and intracluster links, the size of the clusters, and the coupling format on the links. Each quantity has its own role in affecting the network dynamics and, to achieve a stronger synchronizability, we need to balance all these quantities in a global manner. For example, it is recently shown that the mismatch of the two kinds of links, saying fix the number of intercluster links while increasing the number of intracluster links, could suppress synchronizability in cluster networks, despite of the fact that increase of links will make the network closer [5]. While link distribution has been identified as important for network synchronization, the roles of the other two quantities, the cluster size and the coupling format, are still not clear. As pointed out in the previous studies, clusters embedded in a network normally have a wide variety in their size and the largest cluster, which owns a considerable number of intercluster links, has the crucial role in determining the final state of the whole network [6]. Meanwhile, in many biological and neural networks, different clusters often assume different functions and couplings between the different functional clusters are usually asymmetric, i.e., the coupling strength of one direction may weight over the other direction, forming the coupling gradient on the intercluster links [7]. More interestingly, the gradient can be variable in that its weight can be modified by the environment during the system evolution. For example, it is shown that the couplings of the cardiorespiratory interaction changes from a roughly symmetric manner to a nearly unidirectional one during the first 6 months growth of a healthy baby [8]. All these evidences show that, to better understand the

dynamics on cluster networks, we need to take into account of all these network parameters and study their joint effect on the system dynamics. Noticing that by using cluster's size as a proxy for its importance, a topological hierarchy will be formed for the clusters, therefore we are studying the synchronization problem in hierarchical networks.

While gradient coupling has been proven to be prominent in improving synchronizability of non-cluster networks, e.g, the small-world and scale-free networks, its role in cluster networks, to the best of our knowledge, has not been discussed. For non-cluster networks, it has been found that network synchronizability normally can be improved by setting a coupling gradient from the higher degree node to the lower degree node [9]. Imagining each node as a cluster and node degree as the number of intercluster links, it seems reasonable to propose a similar coupling strategy for hierarchical cluster networks: setting gradient on the intercluster links and making it flow from the larger size cluster to the smaller size cluster. Moreover, it is also expected to improve the network synchronizability by simply increasing the gradient, just as what we have done in non-cluster networks. However, as shown in the recent studies, the intra-structure of the clusters adds an additional parameter to the network topology and could bring new features to the network dynamics [5], which indicates that the coupling strategy in cluster networks may have some differences to that of non-cluster networks. Therefore, to better understand the dynamics on cluster networks, we need to consider both the intracluster and intercluster information. Putting in other words, to design an optimal coupling scheme for network synchronization, we need to balance all the four parameters systematically.

In this paper, we develop a theoretical formula to the optimal gradient in hierarchical cluster networks, and explore its dependence to the other network parameters. Our finding shows that gradient indeed can promote network synchronization, but its function is highly related to the other network parameters. Specifically, for network of fixed intra- and intercluster connections, the optimal gradient is proportional to the size difference among the clusters; while for network of fixed cluster size, the optimal gradient depends on the configuration of the two kinds of links. Remarkably, in situations where network changes its parameters as a response to the varying environment, the value of the optimal gradient will also be adjusted accordingly. This kind of nonstationary optimal gradient may provide some clues to the evolution mechanism of some real networks where a variable asymmetric coupling is observed. For example, the change of the cardiorespiratory interaction at the early stage of a baby may suggest that, during this period of growth, some properties of the clusters, e.g. the number of the intra- and intercluster links, are modified by the environ-

ment; keeping up with these modifications, the system updates its coupling gradient accordingly so as to keep with a stronger synchronizability.

We start by constructing a hierarchical network which consists of clusters of different size. Consider a  $N$  nodes and  $M$  clusters network, denote  $n_m$  the size of cluster  $m$  and  $V_m$  the set of nodes it contains ( $m = 1, \dots, M$ ). We connect nodes of the same cluster with probability  $p_s$  and of different clusters with probability  $p_l$ , while keeping  $p_s > p_l$  to ensure the cluster property [5]. To be concrete, we study coupled-map network of the following form:  $\mathbf{x}_{t+1}^i = \mathbf{f}(\mathbf{x}_t^i) - \varepsilon \sum_j C_{i,j} \mathbf{H}[\mathbf{f}(\mathbf{x}_t^j)]$ , where  $\mathbf{x}_{t+1}^i = \mathbf{f}(\mathbf{x}_t^i)$  is a  $d$ -dimensional map representing the local dynamics on node  $i$ ,  $\varepsilon$  is a global coupling parameter,  $C$  is Laplacian matrix representing the couplings, and  $\mathbf{H}$  is a coupling function. For convenience we choose  $C_{i,j} = -A_{i,j}/k_i$  for  $j \neq i$  and  $C_{i,i} = 1$ , with  $k_i$  the degree of node  $i$  and  $A$  the adjacent matrix of the network:  $A_{i,j} = 1$  if node  $i$  and  $j$  are connected and  $A_{i,j} = 0$  if they are not connected. Since the rows of the coupling matrix  $C$  have zero sum, the system permits an exact synchronized solution:  $\mathbf{x}_t^1 = \mathbf{x}_t^2 = \dots = \mathbf{x}_t^N = \mathbf{s}_t$ , where  $\mathbf{s}_{t+1} = \mathbf{f}(\mathbf{s}_t)$  is the synchronous manifold. Without losing the generality, we use logistic map  $f(x) = ax(1-x)$  as the local dynamics and choose  $\mathbf{H}(\mathbf{x}) = x$  as the coupling function. For  $a = 4$ , the single logistic map shows chaotic behavior which is characterized by the Lyapunov exponent  $\ln 2$ . In the following we will adopt this parameter for the local dynamics and study how to improve synchronizability of the coupled map network.

We first consider the situation of two coupled clusters, one of size  $n_1$  and the other one of size  $n_2$ . Constructed with the random model, cluster 1 and cluster 2 consist of  $p_s n_1(n_1 - 1)/2$  and  $p_s n_2(n_2 - 1)/2$  intracluster links respectively, while the number of intercluster links is  $p_l n_2 n_1$ . According to the cluster structure, the adjacent matrix  $A$  can be artificially divided into 4 sub-matrices  $U_{m,l}$ ,  $m, l = 1, 2$ : a  $n_1 \times n_1$  sub-matrix  $U_{1,1}$  consisting of the intracluster links of cluster 1; a  $n_2 \times n_2$  sub-matrix  $U_{2,2}$  consisting of the intracluster links of cluster 2; a  $n_1 \times n_2$  sub-matrix  $U_{1,2}$  consisting of the intercluster links that cluster 1 receives from cluster 2; and a  $n_2 \times n_1$  sub-matrix  $U_{2,1}$  consisting of the intercluster links that cluster 2 receives from cluster 1. To introduce coupling gradient from cluster 1 to cluster 2, we shift partial value  $g \in [0, 1]$  of the nonzero element in  $U_{1,2}$  to the corresponding element in  $U_{2,1}$ , while keeping  $U_{1,1}$  and  $U_{2,2}$  unchanged. The coupling matrix  $C$  then is generated by normalizing the rows of matrix  $A$ ,  $C_{i,j} = -A_{i,j} / \sum_{j=1}^N A_{i,j}$ , while still setting  $C_{i,i} = 1$  for the reason of synchronization solution. According to the shifting, we have  $\sum_{j=1}^N A_{i,j} = k_i - n_2 p_l g$  if  $i \in V_1$  and  $\sum_{j=1}^N A_{i,j} = k_i + n_1 p_l g$  if  $i \in V_2$ . Corresponding to the partitions in  $A$ , after the shifting and normalization operations, the new coupling matrix  $C$  can

also be divided into four parts: a  $n_1 \times n_1$  sub-matrix  $G_{1,2} = C_{i,j}$  with  $i, j \in [1, n_1]$ , representing the intra-connection within cluster 1; a  $n_2 \times n_2$  sub-matrix  $G_{2,2} = C_{i,j}$  with  $i, j \in (n_1, N]$ , representing the intra-connection within cluster 2; a  $n_1 \times n_2$  sub-matrix  $G_{1,2} = C_{i,j}$  with  $i \in [1, n_1]$  and  $j \in (n_1, N]$ , representing the inter-connection that cluster 1 receives from cluster 2; and a  $n_2 \times n_1$  sub-matrix,  $G_{2,1} = C_{i,j}$  with  $i \in (n_1, N]$  and  $j \in [1, n_1]$ , representing the inter-connection that cluster 2 receives from cluster 1. Noticing that nodes of the same cluster have the same degree,  $k_i = n_1 p_s + n_2 p_l = K_1$  when  $i \in V_1$  and  $k_i = n_2 p_s + n_1 p_l$  when  $i \in V_2$ , the nonzero elements in each sub-matrix  $G$  are of the same value:  $g_{1,1} = -1/(k_1 - n_2 p_l g)$  for  $G_{1,1}$ ;  $g_{1,2} = -(1-g)/(k_1 - n_2 p_l g)$  for  $G_{1,2}$ ;  $g_{2,1} = -(1+g)/(k_2 + n_1 p_l g)$  for  $G_{2,1}$ ; and  $g_{2,2} = -1/(k_2 + n_1 p_l g)$  for  $G_{2,2}$ . Therefore the actual gradient generated on the intercluster links is  $\Delta g = g_{1,2} - g_{2,1}$ , which is pointed to cluster 2. Please note that in doing these operations the total coupling cost of the network does not change, what we have done is just to introduce gradient on the intercluster links. In the following we discuss synchronizability of the gradiented matrix  $C$ .

The synchronizability of coupled networks can be evaluated by the method of master stability function (MSF). This method shows that the problem of synchronizability can be divided into two separating issues: the stability of the single dynamics  $\mathbf{F}(\mathbf{x})$  and the eigenvalue spectrum of the coupling matrix  $C$ . For most systems, the single dynamics is only stable within a certain range in the parameter space,  $\sigma \in [\sigma_1, \sigma_2]$ . The network is synchronizable iff all the eigenvalues except the one  $\lambda_1 = 0$ , which corresponding to the synchronous manifold, can be contained within this range after a linear scaling, i.e.  $\lambda_N/\lambda_2 \leq \varepsilon \sigma_2/\sigma_1$ , with  $\lambda_N$  the largest and  $\lambda_2$  the smallest positive eigenvalues of  $C$ , respectively. In other words, the quantity of synchronizability can be characterized by the eigenratio  $R = \lambda_N/\lambda_2$ , with a smaller  $R$  represents a stronger synchronizability. For the logistic map employed here, it is not difficult to prove that  $\sigma_1 = 0.5$  and  $\sigma_2 = 1.5$ . Noticing that for logistic map in most cases we have  $R < \sigma_3/\sigma_1 = 3$ , thus the synchronizability is only determined by  $\lambda_2$ . Since  $\varepsilon \in [0, 1)$ , the synchronization condition thus becomes  $\lambda_2 > \sigma_1 = 0.5$ .

Denoting  $\hat{e}_2 = (e_1, e_2, \dots, e_{n_1}, e_{n_1+1}, \dots, e_N)^T$  the eigenvector associated to  $\lambda_2$  in  $C$ , we have  $\lambda_2 = \hat{e}_2^T C \hat{e}_2 = \sum_{i,j=1}^N e_i C_{i,j} e_j$ . For cluster networks, the elements in  $\hat{e}_2$  have a special distribution:  $e_i = E_1$  for  $i \in [1, n_1]$  and  $e_j = E_2$  for  $j \in [n_1 + 1, N]$  [5]. The two values,  $E_1$  and  $E_2$ , can be derived from the normalization condition  $\hat{e}_2^T \hat{e}_2 = 1$  and the orthogonal condition  $\hat{e}_2^T \hat{e}_1 = 0$  ( $\hat{e}_1$  is the normalized eigenvector associated with  $\lambda_1 = 0$  which describes the synchronous manifold, thus the elements in  $\hat{e}_1$  are identical which are  $1/\sqrt{N}$ ), which yield  $E_1 = -\sqrt{n_2/(n_1 n_2 + n_1^2)}$  and  $E_2 = \sqrt{n_1/(n_1 n_2 + n_2^2)}$  (the sign of  $E_1$  can be either positive or negative given the situa-

tion  $E_1 = -E_2$ ). This will greatly simplify the calculation for  $\lambda_2$ , which now can be written as  $\lambda_2 = \sum_{i=1}^N e_i \{(C_{i,1} + C_{i,2} + \dots + C_{i,n_1})E_1 + (C_{i,n_1+1} + C_{i,n_1+2} + \dots + C_{i,N})E_2\}$ . Noticing the four-part partition of  $C$  and the identical nonzero elements in each part, the calculation can be further simplified as  $\lambda_2 = \sum_{i=1}^{n_1} e_i \{g_{1,1}E_1 \sum_{j=1}^{n_1} A_{i,j} + g_{1,2}E_2 \sum_{j=n_1+1}^N A_{i,j}\} + \sum_{i=n_1+1}^N e_i \{g_{2,1}E_1 \sum_{j=1}^{n_1} A_{i,j} + g_{2,2}E_2 \sum_{j=n_1+1}^N A_{i,j}\}$ . The summation over  $A$  is just the number of intracluster or intercluster links. For node  $i \in V_1$ , on average it has  $n_1 p_s$  intracluster links and  $n_2 p_l$  intercluster links; while if node  $i \in V_2$ , on average it has  $n_2 p_s$  intracluster links and  $n_1 p_l$  intercluster links. Substituting these relations into the calculation, finally we have  $\lambda_2$  for 2-cluster network

$$\lambda_2 = 1 + E_1^2 n_1^2 p_s g_{1,1} + E_2^2 n_2^2 p_s g_{2,2} + E_1 E_2 n_1 n_2 p_l (g_{1,2} + g_{2,1}). \quad (1)$$

Understandings to the terms at the right side of Eq. (1) are straightforward. The unity comes from the diagonal elements in  $C$ , it defines the upper limit for synchronizability (this special case corresponds to the one-way coupled tree-structure network). The second term is contributed by the intra-connection of cluster 1, and the third term is contributed by the intra-connection of cluster 2. The last term is more interesting and worth a special care. It corresponds to the *inter-connection* between the clusters, where the intra-information of both the two clusters are involved. The gradient  $g$  is involved in all the last three terms via  $g_{i,j}$ . While all these three terms contribute negative values to  $\lambda_2$ , their weights are different and can be modified via setting the network parameters. Because the network parameters are complicatedly involved in Eq. (1) (for example,  $g_{i,j}$  are functions of  $n_1$ ,  $n_2$ ,  $p_s$ ,  $p_l$ , and  $g$ ), we can not expect to improve the network synchronizability by simply increasing or decreasing one specific parameter. In particular, when the network topology is fixed, i.e. fixing parameters  $n_1$ ,  $n_2$ ,  $p_s$ , and  $p_l$ , the optimal gradient is determined by equation  $\partial \lambda_2 / \partial g = 0$ , which involves all the parameters nonlinearly.

To visualize the relationship between the parameters, we plot Fig. 1 according to Eq. (1). In Fig. 1(a) we fix parameters  $n_1 = 200$ ,  $n_2 = 100$ , and  $p_l = 0.2$ , while plotting  $\lambda_2$  in the plane of  $p_s$  and  $g$ . A special property about synchronization in cluster network is: increase the number of intracluster links may suppress the synchronizability. This property can be found in Fig. 1(a) at  $g = 0$ , where  $\lambda_2$  decreases monotonically as  $p_s > 0.65$ . Specially, when  $p_s > 0.678$  we have  $\lambda_2 < 0.5 = \sigma_1$ , which means that synchronization is unreachable even with  $\varepsilon = 1$ . Now we increases  $g$  gradually from  $g = 0$  and check its effects to  $\lambda_2$ . It can be found that the synchronizable region in the parameter space of  $p_s$  is significantly enlarged when  $g > 0$ . For examples, when  $g = 0.1$ , the synchronization boundary is extended to  $p_s \approx 0.7$ ; when  $g = 0.9$ , this boundary

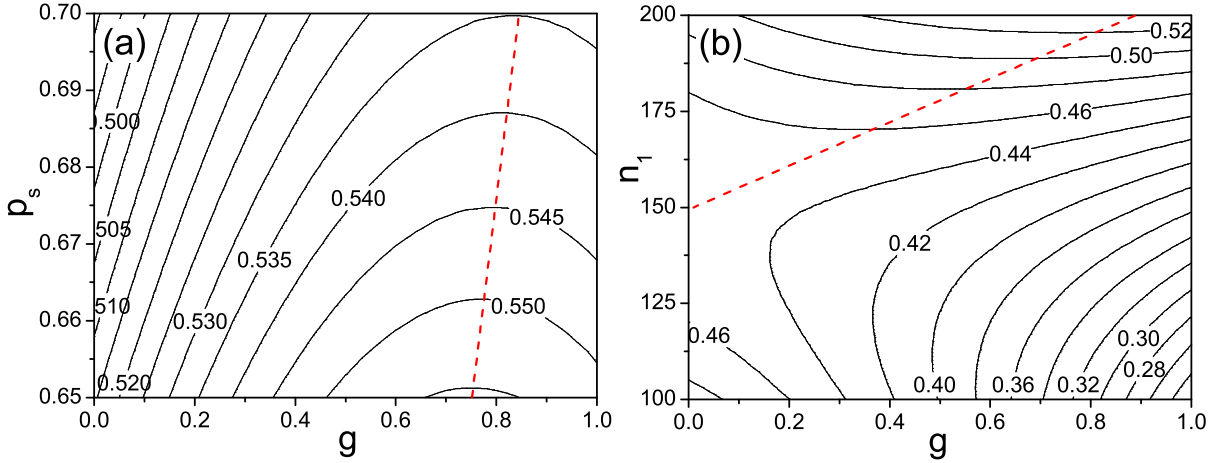


FIG. 1: (Color online). Contour plot of  $\lambda_2$  in the  $(g, p_s)$  plane (a), and in the  $(g, n_1)$  plane (b), for 2-cluster network of 300 nodes and fixed parameter  $p_l = 0.2$ . The other parameters are  $n_1 = 200$  in (a) and  $p_s = 0.7$  in (b).

is further extended to  $p_s \approx 0.8$ . The network synchronizability, however, is not monotonically promoted as the gradient increases. For any given  $p_s$ , there always exists an optimal gradient  $g_o \in [0, 1]$  where  $\lambda_2$  achieves its maximum, while increasing or decreasing  $g$  from  $g_o$  will suppress the synchronizability. In Fig. 1(a) we also plot the location of  $g_o$  as a function of  $p_s$  via setting  $\partial\lambda_2/\partial g = 0$  in Eq. (1). It is found that  $g_o$  shifts from smaller values to larger values monotonically as  $p_s$  increases. This observation indicates that, *comparing to clusters of sparse intra-connection, clusters of dense intra-connection could take more advantage from large gradient.*

With Eq. (1), it is also straightforward to analyze the relationship between the cluster size and the gradient. In Fig. 1(b) we fix parameters  $p_l = 0.2$ ,  $p_s = 0.7$ , and the system size  $N = n_1 + n_2 = 300$ , while plotting  $\lambda_2$  in the plane  $n_1$  and  $g$ . Since the system size is fixed, the change of  $n_1$  will affect the size difference between the two clusters. Noticing that  $n_1 = 150 = N/2$  represents the situation where two clusters have the same size, it is convenient to discuss the two cases  $n_1 > 150$  and  $n_1 < 150$  separately. Since by definition we have assumed that gradient always flows from cluster 1 to cluster 2, therefore when  $n_1 < 150$ , the gradient actually is flowing from the smaller cluster to the larger cluster. In region  $n_1 > n_2$ , i.e.  $n_1 > 150$  in Fig. 1(b), for fixed gradient  $g$ , it is found that  $\lambda_2$  is increased monotonically as  $n_1$  increases. This observation indicates that *clusters of larger size difference take more advantages from large gradient.* In the same region, if we fix

the cluster size  $n_1$  and analyze the dependence of  $\lambda_2$  on  $g$ , it is found that, as  $g$  increases from 0 to 1,  $\lambda_2$  will first increase, then, after an optimal value  $g_o$ , it decreases. The optimal gradient  $g_o$  as a function of  $n_1$  in Fig. 1(b) can also be derived from Eq. 1 by setting  $\partial\lambda_2/\partial g = 0$ , which is plotted in Fig. 1(b) by the dashed line. From the dashed line we get the information that *clusters of larger size difference have a priority in adopting larger gradient than clusters of smaller size difference*. On the contrary, in the region  $n_1 < n_2$ , it is found that  $\lambda_2$  decreases monotonically as  $g$  increases or as  $n_1$  decreases. This observation indicates that, *if the gradient is set with the wrong direction, i.e. from the smaller cluster to the larger cluster, the network synchronizability will be quickly decreased as the gradient increases, and this suppression is further enhanced when the size difference between the clusters is increased*.

Now we are able to give a global understanding to the relationship between the four network parameters and, especially, to identify the multi-role on the effect of coupling gradient in affecting network synchronization. Firstly, the size distribution of the clusters directly determines the gradient direction. To enhance synchronizability, we need to set the gradient starting from the larger cluster and pointing to the smaller cluster. Secondly, when the gradient direction is correctly posed, clusters of large size difference will take more advantage from the gradient. Specifically, the optimal gradient where the maximum synchronizability is achieved is increased as the size difference increases. Thirdly, cluster of dense intra-connection has a higher priority in adopting larger gradient, reflected as the increased  $g_o$  as  $p_s$  increases. Finally, for the fixed network topology, i.e. fixing parameters  $n_1$ ,  $n_2$ ,  $p_s$ , and  $p_t$ , the optimal gradient is an *unique* value between 0 and 1, while its location can be analytically predicted via Eq. (1).

The above discussions are from theoretical analysis, now we provide numerical results to verify our predictions. In Fig. 2(a) we adopt the same set of parameters as in Fig. 1(a), while investigate the variation of  $\lambda_2$  as a function of gradient  $g$  numerically. The gradient effects are clearly shown in Fig. 2(a) as we increase  $g$  from 0 to 1. For curve  $p_s = 0.7$ , when  $g = 0$ , we have  $\lambda_2 \approx 0.49$ , therefore the system is unsynchronizable without gradient. As  $g$  increases,  $\lambda_2$  increases monotonically and at  $g \approx 0.1$  we have  $\lambda_2 \approx 0.5 = \sigma_1$ , from then on the system becomes synchronizable.  $\lambda_2$  increases continuously until the optimal gradient  $g_o \approx 0.8$  is met, where the system takes the full advantages of gradient and achieves the strongest synchronizability  $\lambda_2 \approx 0.54$ . After that increase of  $g$  will decrease  $\lambda_2$ , showing that too large gradient could suppress synchronization. The similar phenomena are also found for curve  $p_s = 0.75$ . In both cases, our theoretical predictions fit the numerical results very well. As we have discussed, cluster with larger  $p_s$  have priority in taking

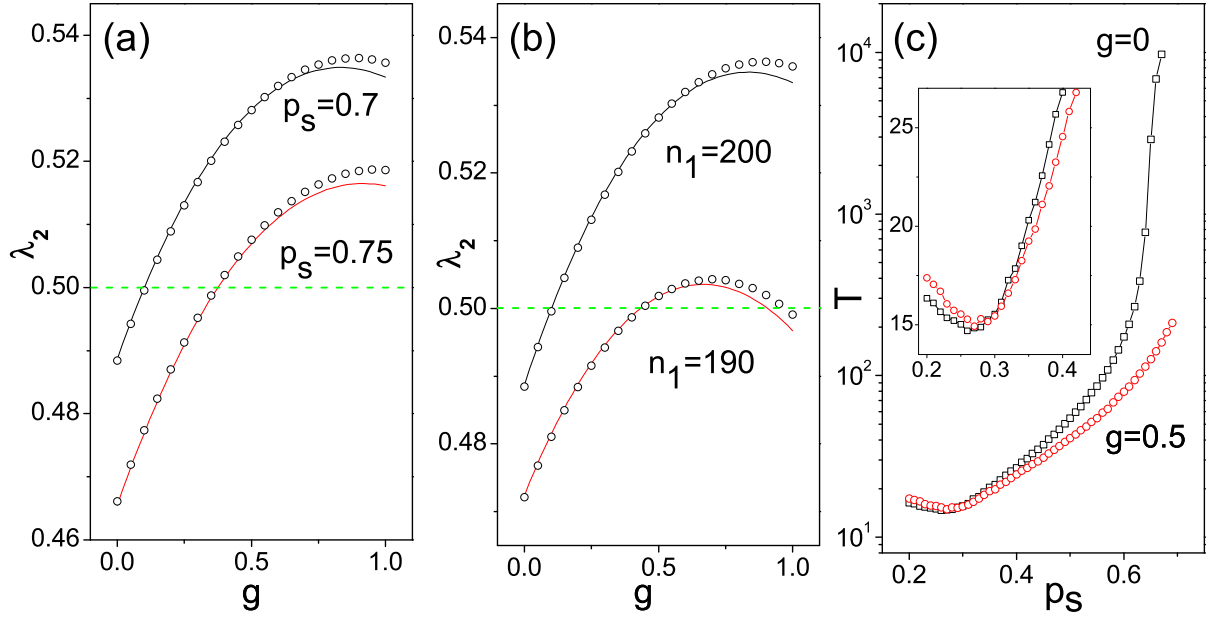


FIG. 2: (Color online). Numerical results on the relationship between  $\lambda_2$  and  $g$  (a)  $\lambda_2$  versus  $g$  by fixing  $p_s$  in Fig. 1(a). (b)  $\lambda_2$  versus  $g$  by fixing  $n_1$  in Fig. 1(b). The corresponding theoretical results are plotted as solid lines. Each data is an average result over 100 network realizations. (c) Transition time versus  $p_s$  for the graded network  $g = 0.5$  and the ungraded network  $g = 0$ . See text for details about the parameters.

large gradient than with smaller  $p_s$ , therefore the optimal gradient in  $p_s = 0.75$  should be larger to that in  $p_s = 0.7$ . This point is also verified by the simulations, where we have  $g_o \approx 1$  in curve  $p_s = 0.75$ , which is larger to the optimal gradient  $g_o \approx 0.8$  found in curve  $p_s = 0.7$ . In Fig. 2(b) we plot the numerical results on the variations of  $\lambda_2$  as a function of  $g$  with the same set of parameters as in Fig. 1(b). Again, the gradient effects and the property of the optimal gradient are well captured by our theoretical predictions. (For asymmetric coupling matrix  $C$ , eigenvector  $\hat{e}_2$  is not exactly orthogonal to eigenvector  $\hat{e}_1$ , i.e.  $\sum_{i=1}^N e_i \neq 0$  for  $\hat{e}_2$ . This error, however, is very small and can be neglected when  $g \approx 0$ . While for  $g \approx 1$  this error induces a small mismatch between the theoretical prediction and the numerical result, as shown at the ends of the two curves.) The gradient effect is also reflected in the transition time  $T$  in network synchronization. Here the transition time is defined as the moment when  $\sum_{i=1}^N |(x^i - \langle x \rangle)|/N < \delta = 10^{-5}$ , with  $\langle x \rangle = \sum_{i=1}^N x^i/N$  the mean value of the trajectories. For the same set of parameters as in Fig. 1(a), we compare in Fig. 2(c) the transition times between the cases of  $g = 0$  and  $g = 0.5$

for varying  $p_s$ . The comparison is carried within region  $p_s \in (0.2, 0.678)$ , since in this region the system is synchronizable for both cases. As can be seen from Fig. 2(c), the gradiented network has a clear advantage over the unweighted one at large  $p_s$ . This advantage, however, trails off as  $p_s$  decreases and, at about  $p_s \approx 0.28$ , these two networks have the same transient time. If we further decrease  $p_s$  from  $p_s = 0.28$ , the opposite situation happens: gradiented network has longer transient time than ungradiented one. This observation is in consistency with our theoretical predictions that gradient will promote synchronization only for clusters of dense intra-connections, while for clusters of sparse intra-connections gradient may suppress synchronization. As shown in the inset plot of Fig. 2(c), when  $p_s < 0.28$ , the transition time for the gradient network at  $g = 0.5$  is longer to the ungradiented one.

The theory we have established for 2-cluster networks can be extend to the situation of many-cluster networks. Consider a  $M$ -cluster network constructed with the random model, denote  $n_m$ ,  $m = 1, \dots, M$  the size of cluster  $m$  and  $V_m$  the set of nodes it includes. Initially the coupling matrix reads  $C_{i,j} = -A_{i,j}/k_i$ , with  $A_{i,j}$  the adjacency matrix and  $k_i$  the degree of node  $i$ . According to the cluster structure, matrix  $A$  can be divided into  $M^2$  sub-matrices  $U_{m,l}$ ,  $m, l = 1, \dots, M$ . The sub-matrix  $U_{m,l}$  has  $n_m$  rows and  $n_l$  columns. When  $m \neq l$ , it represents the inter-connections between cluster  $m$  and cluster  $l$ ; when  $m = l$ , it represents the intra-connections within cluster  $m$ . To introduce gradient from cluster  $m$  to cluster  $l$ , we decrease each nonzero element in sub-matrix  $U_{m,l}$  by value  $g$  and add it to the corresponding element in sub-matrix  $U_{l,m}$ . We do this shifting for all the  $M(M - 1)$  sub-matrices  $U_{m,l}$  ( $m \neq l$ ) while keeping the gradient be always pointing to the smaller cluster. The coupling matrix  $C$  then is generated from  $A$  by normalizing its rows  $C_{i,j} = -A_{i,j}/\sum_{j=1}^N A_{i,j}$ , again we set  $C_{i,i} = 1$  for the reason of synchronization solution. After the shifting operations, for node  $i \in V_m$  we have  $\sum_{j=1}^N A_{i,j} = k_i + p_l g(\sum_l n_l - \sum_{l'} n_{l'})$ , with  $l$  the set of clusters of  $n_l > n_m$ , while  $l'$  the set of clusters of  $n_{l'} < n_m$ . Corresponding to the partitions in  $A$ , after the shifting and normalization operations, the new coupling matrix  $C$  can also be divided into  $M^2$  sub-matrices  $G_{i,j}$  ( $i, j = 1, \dots, M$ ). Noticing that nodes of the same cluster have the same degree,  $k_i = n_m p_s + (N - n_m) p_l = K_m$  for  $i \in V_m$ , the nonzero elements in each sub-matrix  $G_{i,j}$  have the same value:  $g_{i,j} = -1/\{K_m + p_l g(\sum_l n_l - \sum_{l'} n_{l'})\}$ . The elements of eigenvector  $\hat{e}_2 = (e_1, e_2, \dots, e_N)^T$  are also organized into  $M$  groups, with elements within the same group have the same value, i.e.  $e_i = E_m$  for  $i \in V_m$ . By the special property of  $G$  and  $\hat{e}_2$ , we have  $\lambda_2 = \hat{e}_2^T G \hat{e}_2 = \sum_{i=1}^N e_i \sum_{j=1}^N e_j G_{i,j} = \sum_{m=1}^M n_m E_m \sum_{m'=1}^M n_{m'} E_{m'} g_{m,m'}$ . Considering the normalization condition  $\hat{e}_2^T \hat{e}_2 = 1$ , finally we have  $\lambda_2$  for  $M$ -cluster network

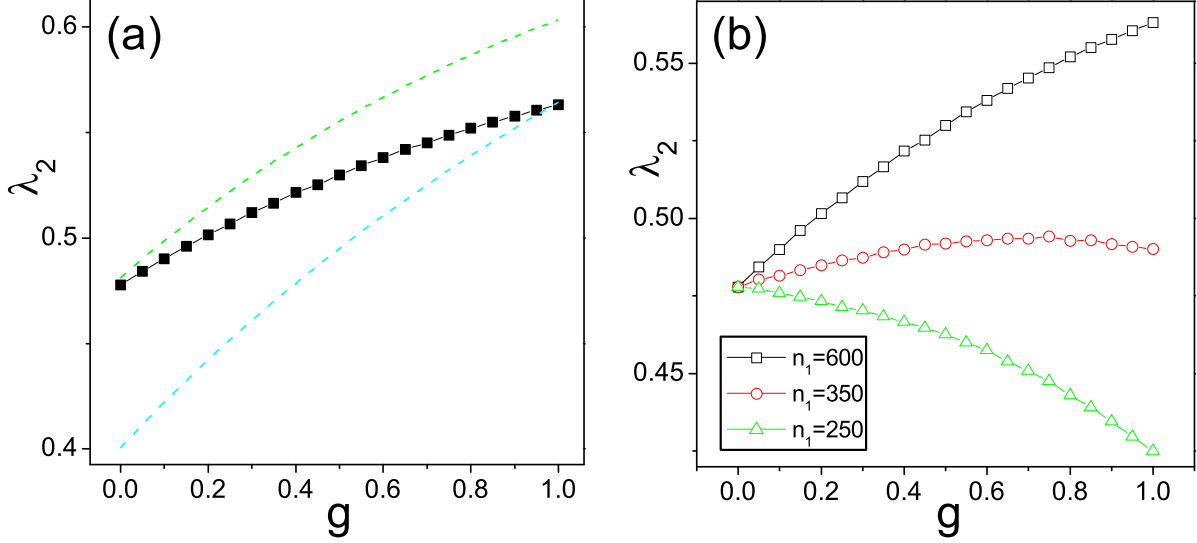


FIG. 3: (Color online). For 3-cluster network of parameters  $p_l = 0.15$ ,  $p_s = 0.7$ ,  $n_2 = 200$ ,  $n_3 = 100$ . (a)  $\lambda_2$  versus  $g$  when  $n_1 = 600$ . The two dashed curves represent the theoretical prediction of  $\lambda_2$  by using  $E_m$  in the limiting cases of  $g = 0$  (the upper curve) and  $g = 1$  (the lower curve). (b)  $\lambda_2$  versus  $g$  for different  $n_1$ . It is found that, as  $n_1$  decreases, the optimal gradient decreases. Each data is an average result of 100 network realizations.

$$\lambda_2 = 1 + \sum_{m=1}^M E_m^2 n_m^2 p_s g_{m,m} + \sum_{m,m'=1}^M E_m E_{m'} n_m n_{m'} p_l (g_{m,m'} + g_{m',m}). \quad (2)$$

As an example, we study the network of 3 clusters. To predict  $\lambda_2$  by Eq. (2), we first need to determine two sets of values,  $g_{m,l}$  and  $E_m$ ,  $m = 1, 2, 3$ . While  $g_{m,l}$  can be uniquely determined by the network parameters, i.e.  $g_{m,l} = g_{ml}(n_1, n_2, n_3, p_s, p_l, g)$ , the values of  $E_m$ , different to the situation of 2-cluster networks, are not unique and can not be derived explicitly. Even so, we are still able to characterize the behavior of  $\lambda_2$  in a quantitative way by considering the two limiting cases,  $g = 0$  and  $g = 1$ , while  $\lambda_2$  of other values of  $g$  should be within the boundaries set by the limiting cases. The values of  $E_m$  for  $g = 1$  can be explicitly given, since we have  $E_1 = 0$ , while  $E_2$  and  $E_3$  can be determined by the normalization and orthogonal conditions. However, when  $g = 0$ , we can only get  $E_m$  by simulations. In Fig. 3(a) we plot  $\lambda_2$  as a function of  $g$  for clusters of size:  $n_1 = 600$ ,  $n_2 = 200$ ,  $n_3 = 100$ . It can be seen that, as  $g$  increases, the network changes from the unsynchronizable state of  $\lambda_2 < 0.5$  to the synchronizable state  $\lambda_2 > 0.5$ . It is also found

that the value of  $\lambda_2$  exists between the two boundaries set by the extreme cases. To investigate the effects of cluster size in affecting the optimal gradient, in Fig. 3(b) we plot  $\lambda_2$  as a function of  $g$  for different  $n_1$ . It is found that the optimal gradient  $g_o$  shifts its location as  $n_1$  varies: for  $n_1 = 600$ , we have  $g_o \approx 1$ ; for  $n_1 = 350$ , we have  $g_o \approx 0.7$ ; while for  $n_1 = 250$ , we have  $g_o \approx 0$ , which means that, if clusters are of the similar size, increase of  $g$  will suppress synchronization.

In summary, we have investigated the synchronization problem in hierarchical cluster networks, and analyzed the joint effects of the network parameters in affecting the network synchronizability. Coupling gradient between clusters plays a significant role in promoting network synchronization, but its efficiency is modulated by the other parameters. For network of given topology and fixed coupling cost, the optimal gradient, where the strongest network synchronizability is achieved, can be predicted analytically. Our study may give insight to the organization of some real networks where units are grouped into clusters of different size and synchronization is important for the network functions, for example, the cardiorespiratory network.

X.G. Wang acknowledges the great hospitality of Arizona State University, where part of the work was done during a visit. Y.-C. Lai and L. Huang were supported by NSF under Grant No. ITR-0312131 and by AFOSR under Grant No. FA9550-06-1-0024 and No. F49620-01-01-0317.

- 
- [1] M. Girvan and M.E.J. Newman, Proc. Natl. Acad. Sci. U.S.A. **99**, 7821 (2002).
  - [2] E. Ravasz, A.L. Somera, D.A. Mongru, Z. Oltvai, and A.-L. Barabasi, Science **297**, 1551 (2002); R. Milo, S. Shen-Orr, S. Itzkovitz, N. Kashtan, D. Chklovskii, and U. Alon, Science **298**, 824 (2002); V. Spirin and L.A. Mirny, Proc. Natl. Acad. Sci. U.S.A. **100**, 12123 (2003).
  - [3] D.J. Watts and S.H. Strogatz, Nature 393, 440 (1998); E. Rodriguez, N. George, J.-P. Lachaux, J. Martinerie, B. Renault, and F.J. Varela, Nature 397, 430 (1999); M. Barahona and L.M. Pecora, Phys. Rev. Lett. **89**, 054101 (2002); T. Nishikawa, A.E. Motter, Y.-C. Lai, and F.C. Hoppensteadt, Phys. Rev. Lett. **91**, 014101 (2003); S. Boccaletti and L.M. Pecora, Chaos **16**, 015101 (2006); A.E. Motter, M.A. Matias, J. Kurths, and E. Ott, Physica D **224**, 7 (2006).
  - [4] P.N. McGraw and M. Menzinger, Phys. Rev. E **72**, 015101 (2005); A. Arenas, A. Diaz-Guilera, and C.J. Perez-Vicente, Phys. Rev. Lett. **96**, 114102 (2006).
  - [5] K. Park, Y.-C. Lai, S. Gupte, and J.-W. Kim, Chaos **16**, 015105 (2006); L. Huang, K. Park, Y.-C. Lai, L. Yang, and K. Yang, Phys. Rev. Lett. **97**, 164101 (2006).

- [6] A. Wagner and D.A. Fell, Proc. R. Soc. London Ser. B **268**, 1803 (2001); E. Ravasz, A.L. Somera, D.A. Mongru, Z.N. Oltvai, and A.-L. Barabasi, Science 297, 1551 (2002); C. Zhou and J. Kurths, Phys. Rev. Lett. 96, 164102 (2006).
- [7] M. Yoshioka and M. Shiino, Phys. Rev. E **55**, 7401 (1997); J. Bragard, S. Boccaletti, and H. mancini, Phys. Rev. Lett. 91, 064103 (2003).
- [8] M.G. Rossenblum, L. Cimponeriu, A. Bezerianos, A. Patzak, and R. Mrowka, Phys. Rev. E 65, 041909 (2002).
- [9] A.E. Motter, C. Zhou, and J. Kurths, Europophys. Lett. **69**, 334 (2005); M. Chavez, D.-U. Hwang, A. Amann, H.G.E. Hentschel, and S. Boccaletti, Phys. Rev. Lett. **94**, 218701 (2005); D.-U. Hwang, M. Chavez, A. Amann, and S. Boccaletti, Phys. Rev. Lett. **94**, 138701 (2005); C. Zhou, A.E. Motter, and J. Kurths, Phys. Rev. Lett. **96**, 034101 (2006); T. Nishikawa and A.E. Motter, Phys. Rev. E **73**, 065106 (2006).